

Synthesis and Characterisation of Nano Zero-Valent Iron for the Reduction and Immobilisation of Cr(VI) in Water Resources

M. Stojchevski,^{a*} S. Kuvendziev,^a Z. Bozinovski,^b P. Makreski,^c P. Paunović,^a
M. Marinkovski,^a and K. Lisichkov^a

^aSs. Cyril and Methodius University in Skopje, Faculty of Technology and Metallurgy, Ulica Rugjera Boskovica 16, 1000 Skopje, R. N. Macedonia

^bEko Bio Link, Ulica Petra Deljana 3-1/4, 1000 Skopje, R. N. Macedonia

^cSs. Cyril and Methodius University in Skopje, Faculty of Natural Sciences and Mathematics, Institute of Chemistry, Arhimedova ulica 5, 1000 Skopje, R. N. Macedonia

This work is licensed under a
Creative Commons Attribution 4.0
International License



Abstract

Nano zero-valent iron (nZVI) was synthesised through the chemical reduction of Fe(III) ions using iron(III) chloride and sodium borohydride solutions under atmospheric conditions. Structural and chemical characterisation of nZVI was performed using scanning electron microscopy (SEM), X-ray powder diffraction (XRPD), energy dispersive X-ray fluorescence spectrometry (EDXRF), thermogravimetric/differential thermal analysis (TGA/DTA), specific surface area analysis (SSA), and ultraviolet-visible spectroscopy (UV/Vis). The synthesised iron exhibited a zero oxidation state and a nearly one-dimensional morphology. The zero-valent iron nanoparticles with a body-centred cubic crystal structure remained chemically stable for several months. The mean diameter of individual nanoparticles was less than 60 nm, with an SSA of 23.79 m² g⁻¹. The synthesised nZVI was applied for the catalytic reduction of Cr(VI) in an aqueous solution. The effects of contact time and initial nZVI concentration on the efficiency of Cr(VI) removal from aqueous solution were investigated. The removal efficiency reached 44.2, 74.6, and 94.5 % after 300 min at initial nZVI concentrations of 20, 40, and 60 mg l⁻¹, respectively. This study suggests that the obtained nZVI is an environmentally friendly and effective reducing agent for treating wastewater and groundwater contaminated with hexavalent chromium.

Keywords

Nano zero-valent iron, synthesis, characterisation, Cr(VI) removal

1 Introduction

Pollution is one of the most significant challenges today, as it affects all crucial aspects of the environment, especially the hydrosphere.¹ Natural and synthetic organic compounds, such as phosphorus and nitrogen compounds, nitrates, industrial colourants, and pesticides, are the most common pollutants found in the hydrosphere, along with inorganic pollutants, particularly heavy metals and metalloids.^{2,3} Heavy metals are persistent, highly toxic, and non-biodegradable pollutants.⁴ Among them, chromium's toxicity depends on its oxidation state and duration of exposure. Trivalent chromium [Cr(III)] and hexavalent chromium [Cr(VI)] are the most stable forms of chromium in the environment, with Cr(III) being about 1000 times less toxic than Cr(VI).⁵ Therefore, the removal of Cr(VI) from water resources is a major concern.

Nano zero-valent iron (nZVI) is an efficient remediation agent that can be used to address various environmental issues, such as soil and groundwater remediation, mainly due to its particle size ranging from 60 to 70 nm, a specific area of 10–30 m² g⁻¹, and a high tendency to oxidise. nZVI is a highly reactive metal with a standard reduction potential of $E^0 = -0.44$ V (Fe(II)/Fe).^{6–9} However, its performance is limited due to the agglomeration, surface passivation, pH sensitivity, and sensitivity to dissolved oxygen

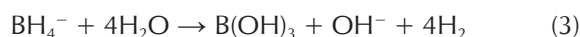
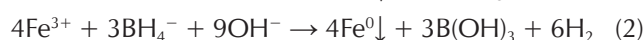
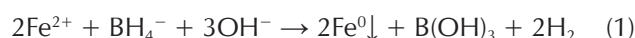
in the environment. To mitigate these drawbacks, various methods for surface modifications and coating of nZVI have been developed and applied.^{10–12}

Nano zero-valent iron has been successfully applied to treat groundwater and wastewater contaminated with heavy metals such as Pb(II), Zn(II), Cd(II), Co(II), Ni(II), arsenic, nitrates, colourants, halogenic organic compounds, antibiotics, pesticides, etc.^{13–21} The removal of pollutants using nZVI typically involves two phases: the reduction of pollutants through direct electron transfer from nZVI, and the subsequent oxidation of nZVI to Fe(II) or Fe(III), where the iron ions are generally removed as Fe(OH)₃.²²

Recently, various physical and chemical methods have been implemented for nZVI synthesis. When milling is used as a physical process, nZVI is prone to oxidation due to the presence of water, oxygen, or other oxidants, resulting in a significant loss of nZVI. As a result, this process is not recommended when the goal is to obtain Fe(0) nanoparticles with particle sizes less than 100 nm.²³ Thermal reduction of iron compounds is another potential and cost-effective method for nZVI synthesis.²⁴ This process occurs at relatively high temperatures, and gases such as H₂, CO, and CO₂ produced during the thermal decomposition of carbon-based materials are usually used as reducing agents.²⁵ To date, electrolysis is a highly efficient and relatively simple method commonly used in nZVI synthesis. It involves the reduction of Fe(II) or Fe(III) ions in a solution by applying electricity, resulting in the deposition of nZVI.²⁶

* Corresponding author: Martin Stojchevski, MSc
Email: martin@tmf.ukim.edu.mk

The reduction of Fe(II) or Fe(III) ions in solutions with NaBH_4 is a chemical method for nZVI preparation. The reduction process follows Eqs. (1)–(3):²⁶



This method of nZVI synthesis is relatively complex, involving several processes such as particle nucleation, particle growth, and nZVI agglomeration. Since Fe oxidation should be avoided, production is mainly guided under inert conditions.²⁷ However, ensuring inert conditions increases the process cost, so this method is commonly performed under atmospheric conditions, often producing nZVI with a particle size of 10 to 100 nm.²⁸ The economic efficiency of the process can be improved by the appropriate utilisation of the hydrogen generated during NaBH_4 reaction and hydrolysis.²⁹ Particle size can also be reduced using high-power ultrasonication during synthesis.³⁰

Recently, nZVI synthesis processes following green chemistry principles have become increasingly attractive due to their numerous advantages. These processes are environmentally friendly, non-toxic, and safe, often utilising plants, seeds, fruit extracts, and other natural materials. Typically performed at low pressures and temperatures, these methods are energy-efficient and easy to implement.^{31–33} The performance of nZVI largely depends on factors such as synthesis method, particle size, specific surface area, agglomeration, storage method, and purity. Therefore, the characterisation of nZVI is prescribed as a mandatory step.⁸

This study aimed to synthesize pure zero-valent iron nanoparticles and evaluate their performance using various instrumental techniques for characterization. The main objective was to produce a low-cost, environmentally friendly, and highly efficient material with suitable physicochemical properties for addressing local Cr(VI) contamination in groundwater through an *in situ* remediation system.

2 Experimental

2.1 Synthesis of nano zero-valent iron

Nano zero-valent iron was synthesised through the chemical reduction of Fe(III) ions using ferric chloride and sodium borohydride solutions under atmospheric conditions. The nZVI was produced in a lab-scale reactor according to the method described by Yuvakkumar *et al.*,³⁴ with specific modifications to obtain application-ready material. For this purpose, 2.5 g of iron(III) chloride hexahydrate (Merck, for analysis) was dissolved in a mixture of 96 % ethanol (Ph.Eur., Alkaloid) and deionised water. The mixture was stirred in a 1000-ml laboratory batch glass reactor using a magnetic stirrer until iron(III) chloride hexahydrate was fully dissolved. Separately, an aqueous solution of 0.25 M sodium borohydride was prepared in a laboratory bottle. The NaBH_4 solution was stirred for approximately 1 min with a vortex mixer.

The solution was then transferred to a separatory funnel and added dropwise to the FeCl_3 solution (2 drops *per* second). The reaction was performed at a stirring speed of 300 rpm under atmospheric conditions. After the complete addition of the NaBH_4 solution, the reaction mixture was left for an additional 15 min. The synthesis process of nZVI is illustrated in Fig. 1.

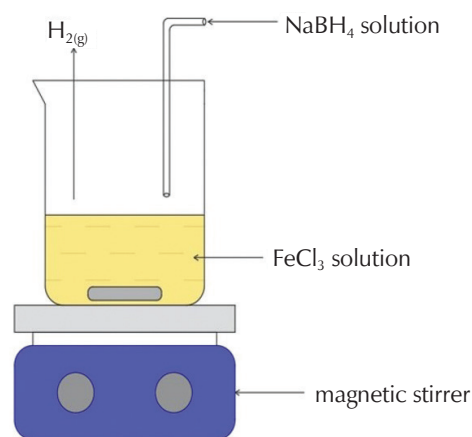


Fig. 1 – Schematic diagram of the nZVI synthesis process

After synthesising nZVI, the next crucial step was to separate the nZVI from the liquid reaction medium. This was accomplished through vacuum filtration, where the black solid nZVI nanoparticles were collected on filter paper (Macherey-Nagel MN640 DE). The nZVI was then washed with a solution of ethanol and deionised water to remove residual NaCl. A subsequent wash with ethanol was performed to remove water and other products. The nZVI nanoparticles were then dried for 20 h in a vacuum desiccator at a pressure of 20 kPa and a temperature of 50 °C. Once dried, the nZVI was stored in a vacuum bag until further analysis.

2.2 Characterisation of nZVI

The structural and chemical characterisation of nZVI was conducted using scanning electron microscopy (SEM), X-ray powder diffraction (XRPD), energy dispersive X-ray fluorescence spectrometry (EDXRF), thermogravimetric/differential thermal analysis (TGA/DTA), specific surface area analysis (SSA), and ultraviolet-visible spectroscopy (UV/Vis).

SEM analysis of the synthesized nZVI was performed using the JSM-IT200 scanning electron microscope equipped with a fully integrated energy-dispersive X-ray spectrometer (EDS). An untreated nZVI sample was examined under high vacuum at a voltage of 15 or 20 kV to determine the morphology and size of the synthesised particles. The EDS spectrum was recorded at a selected line on the surface of the nZVI to determine the elemental composition of the sample.

The thermal properties of the synthesized nZVI were analysed using a PerkinElmer PYRIS Diamond Thermogravimetric/Differential Thermal Analyzer (TGA/DTA/DTG). Approximately 8.4 mg of nZVI was heated from 25 to 850 °C at a rate of 20 °C min⁻¹ under air purging. TGA was carried out to determine the thermal stability of nZVI by monitoring the weight change as a function of temperature, while DTA was employed to investigate the transformations in the sample.

The chemical composition and crystalline properties of the nZVI were analysed using a Rigaku Ultima IV X-ray diffractometer. An X-ray tube set at a voltage of 40 kV and electricity of 30 mA was applied to generate CuK α radiation ($\lambda = 0.154178$ nm), with a K β filter in place. The XRPD diffractogram of nZVI was recorded in the 20–70° (2 θ) range at a scan rate of 5° min⁻¹ on a high-resolution D/tex Ultra high-speed 1D detector.

The elements present in the investigated nanoparticles were identified and quantified using the Thermo Scientific ARL QUANT'X EDXRF analyser, equipped with an Rh anode X-ray tube and high-performance silicon drift SDD detectors. EDXRF, as a non-destructive analytical technique, was employed due to its high efficiency and sensitivity in trace analysis. An as-prepared sample of nZVI was measured under air. Approximately 1.9 g of nZVI was used to determine the elemental composition.

The specific surface area of the produced material was determined using the Brunauer–Emmett–Teller (BET) method. Approximately 1 g of nZVI was dried at 200 °C for 120 min under argon purging to remove surface moisture. The dried sample was then transferred into a glass tube and analysed using a Micromeritics TriStar II 3020 surface area and porosity analyser. The measurement was conducted with nitrogen gas at –196 °C under controlled pressure, and the BET surface area value was calculated from the nitrogen adsorption isotherm using the instrument's software.

The UV/Vis spectrum of nZVI was recorded using Spectroquant® Prove 600 UV/VIS spectrophotometer. For this analysis, 10 mg of nZVI was placed in a 50-ml flask containing absolute ethanol (Supelco), and subjected to ultrasonic treatment at a frequency of 40 kHz in an ultrasonic bath. After 120 min, the sample was filtered through a 0.45 μ m pore-sized filter. The baseline was automatically adjusted using absolute ethanol as a blank. The spectrum was recorded over 190 to 500 nm, with peak detection set at 0.05 and $\Delta\lambda$ at 1 nm.

The synthesised nZVI was packed in a vacuum-sealed plastic bag after the drying process, and stored in a dark environment at room temperature. The stability of nZVI stored under these conditions was an important analysis for performance. The presence of trace water in nZVI, as well as its high reactivity with oxygen, can potentially alter the zero oxidation state of nZVI. The Fe(0) loses electrons and forms oxides or hydroxides, reducing its effectiveness as a reducing agent. Among several available methods to analyse the chemical stability of nZVI, its efficiency in removing Cr(VI) from aqueous solutions was tested using the batch experimental method. For this purpose, 2000 ml

of hexavalent chromium solution (2 mg l⁻¹) was prepared using a chromate standard solution (Merck, 1000 mg l⁻¹ CrO₄) and deionised pure water (conductivity below 0.5 μ S cm⁻¹). The initial pH and temperature of the Cr(VI) solution were 7 and 20 °C, respectively. The initial pH of the solution was adjusted to 7 using a 0.1 M solution of HCl or a 0.1 M solution of KOH. The Cr(VI) solution was stirred with a magnetic stirrer at a speed of 1000 rpm under atmospheric conditions. A total of 80 mg of nZVI was added to the Cr(VI) solution (initial concentration of nZVI was 40 mg l⁻¹). Samples of 5 ml were taken at 0, 30, and 60 min and filtered through a 0.45 μ m membrane filter. The concentration of Cr(VI) was measured photometrically using the chromium (VI) test (Merck, Chromate test (chromium VI) method) at 540 nm and Spectroquant® Prove 600 UV/VIS spectrophotometer. The stability of nZVI was monitored over 90 days, with reduction tests conducted every 15 days.

The removal efficiency of Cr(VI) by nZVI was mathematically calculated using the Eq. (4).

$$R = \frac{C_0 - C_t}{C_0} \cdot 100 \quad (4)$$

R is the removal efficiency of Cr(VI) (%), and C₀ and C_t are the initial and time-specific concentrations (mg l⁻¹) of Cr(VI), respectively.

2.3 Removal (reduction and immobilisation) of Cr(VI) by nZVI

The synthesised nZVI was applied as a reducing agent for the treatment of Cr(VI)-contaminated water. Cr(VI) was removed from the aqueous solution by nZVI in a glass beaker under atmospheric conditions. The effects of contact time and initial nZVI concentration were investigated. For this purpose, 2000 ml of Cr(VI) solutions were prepared using a chromate standard solution and deionised pure water. The catalytic reduction process was performed with initial nZVI concentrations of 20, 40, and 60 mg l⁻¹ and contact times ranging from 0 to 300 min. The initial solution pH was adjusted to 7 using a 0.1 M solution of HCl or a 0.1 M solution of KOH, and the initial concentration of Cr(VI) was 2 mg l⁻¹. The Cr(VI) removal process by nZVI was performed at a mixing speed of 1000 rpm and a temperature of 20 °C. The samples were filtered through a 0.45 μ m membrane filter for analysis. The concentration of Cr(VI) was measured using the photometric method described in Section 2.2. The percent removal of Cr(VI) was calculated using Eq. (4).

3 Results and discussion

The SEM photographs of the synthesized nZVI using the reduction method of Fe(III) ions with sodium borohydride as a reducing agent under atmospheric conditions are shown in Fig. 2. The microphotographs show that the iron nanoparticles possessed almost one-dimensional (1D) morphology, and their average diameter being less than 60 nm.

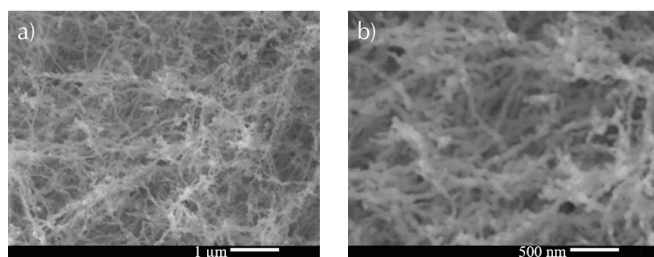


Fig. 2 – SEM photographs of nZVI: a) $\times 20000$ magnification, and b) $\times 40000$ magnification

The EDS spectrum obtained at a selected line on the surface of the nZVI is presented in Fig. 3. Strong lines characteristic of iron were observed in the spectrum. In addition to iron, oxygen was also detected, which is likely due to the formation of a very thin iron oxide (Fe_xO_y) shell around the cores of the nZVI particles. This phenomenon has been documented in previous studies.^{35,36} The EDS analysis confirms that the iron in the sample was produced in the zero oxidation state. SEM analysis confirmed the nanochain morphology of the obtained Fe.

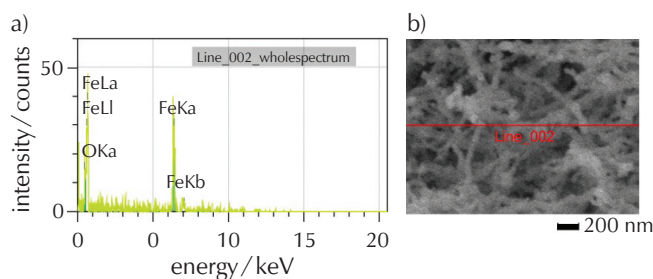


Fig. 2 – EDS spectrum of nZVI recorded at the selected line on the nZVI surface: a) EDS spectrum of nZVI, and b) selected line of nZVI

The results of thermogravimetric and differential thermal analyses of nZVI under a controlled atmosphere and temperature are shown in Fig. 4. The TG curve represents the weight variation of nZVI as a function of temperature. It demonstrates that the weight of nZVI decreased linearly up to ≈ 100 °C. This mass loss was attributed to the evaporation of water: 1) physically adsorbed water on the sample, and 2) residual water from the solvent used in the process of synthesis (ethanol 96 %). Between 100 °C to 850 °C, the weight of nZVI increased almost linearly, suggesting the oxidation of Fe(0) to Fe(II) and Fe(III). The total mass yield of 30 % corresponds to the stoichiometric Fe/O ratio in hematite (Fe_2O_3), confirming that the analysed material in the thermal analysis was pure zero-valent iron. This also indicates the high electron-donating tendency of nZVI. The exothermic peak observed in the DTA curve at 790 °C could be attributed to the oxidation of Fe(II) to Fe(III).

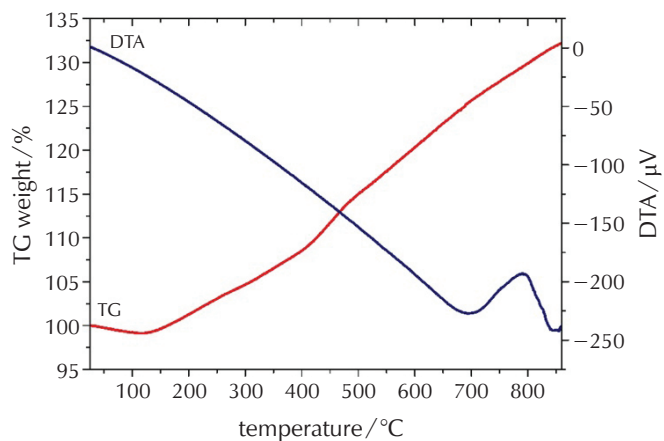


Fig. 4 – TG and DTA curves of nZVI

The XRPD diffractogram of nZVI is presented in Fig. 5. The X-ray diffraction pattern confirmed that the synthesised iron was crystalline and existed in a zero oxidation state. The main peak at $2\theta = 44.7^\circ$ (100) and an additional peak at $2\theta = 65.04^\circ$ (200) indicated that the synthesised iron possessed a body-centred cubic (bcc) crystal structure, confirming the presence of predominantly alpha iron ($\alpha\text{-Fe}^0$).

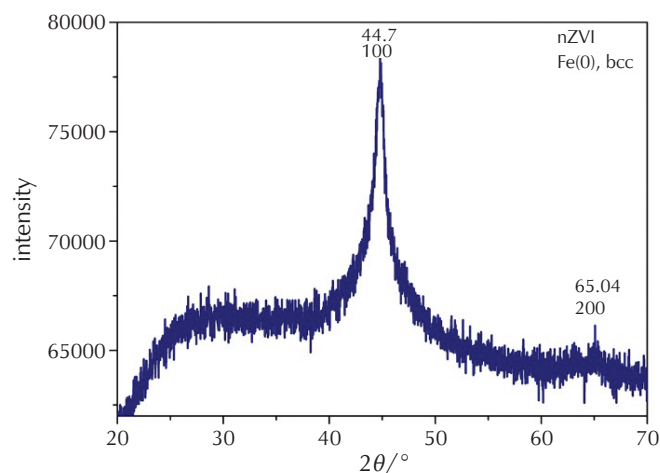


Fig. 5 – XRPD diffractogram of nZVI

XRPD analysis confirmed the successful synthesis of nZVI consistent with the results from the TGA/DTA analysis. No iron oxide was detected, aside from zero-valent iron, verifying that the oxygen detected in the EDS spectrum originated from the thin iron oxide (Fe_xO_y) shell formed around the cores of the nZVI particles. The minimal amount of iron oxide in the sample indicated that the surface layer of iron oxide was too thin.

The EDXRF analysis results, presented in Table 1, further confirmed that the obtained material was pure iron with only negligible impurities.

Table 1 – EDXRF analysis of nZVI

Element	Mass percentage / %
Fe	99.8
P	0.112
Ca	0.0468
Cl	0.0412

The amount of nitrogen gas adsorbed (mmol g^{-1}) as a function of relative pressure (absolute/saturation pressure) is presented in Fig. 6. The BET surface area of the nZVI was calculated to be $23.79 \text{ m}^2 \text{ g}^{-1}$, suggesting that the synthesized material had a large specific surface area, enhancing its effectiveness in removing heavy metals from contaminated water resources.

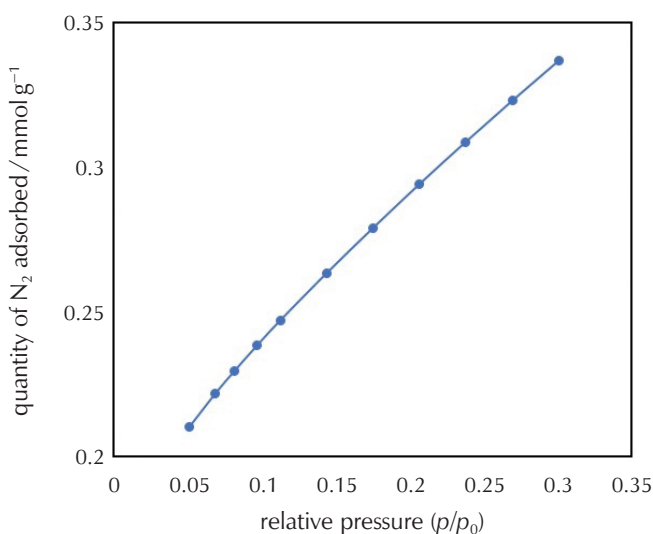


Fig. 6 – BET surface area analysis of nZVI

The physical and chemical properties of metal nanoparticles differ from their macro equivalents. Metal nanoparticles exhibit optical, magnetic, and electronic properties that are highly dependent on particle size and shape. The optical properties are correlated with quantum effects, due to the high density of free electrons. In zero-valence iron nanoparticles, the valence and conduction bands overlap, so there are delocalised electrons in the conduction band that move freely through the crystal lattice. These free electrons resonate with electromagnetic UV/Vis waves, producing surface plasmon resonance. In metal chains and nanotubes, such as the synthesized nZVI particles, the plasma wave propagates along the arrays through the sequential interaction of the particles.^{37–39}

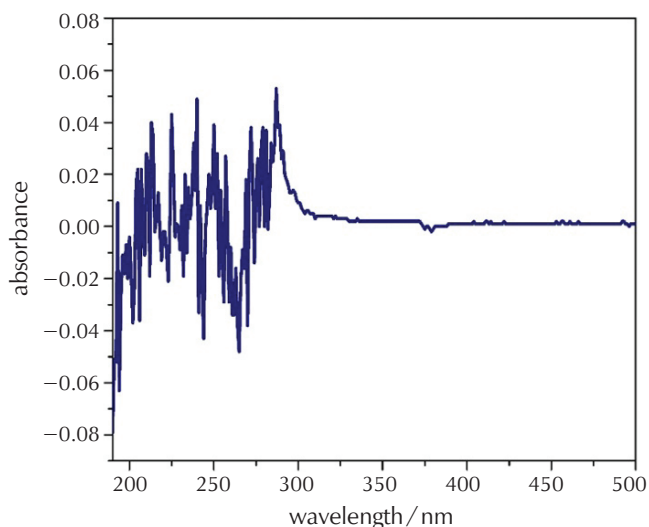


Fig. 7 – UV/Vis spectrum of nZVI

The UV/Vis pattern of the synthesised nZVI is shown in Fig. 7. Narrow absorption peaks were observed in the UV range from 190 to 290 nm, consistent with similar findings in other studies.^{6,16} Analysis of the UV/Vis spectrum confirmed the presence of nZVI particles in the studied samples, indicating the successful synthesis of the desired material. The characteristic peak wavelengths further verified the presence of nZVI. Multiple peaks in the UV/Vis spectrum were expected in this heterogeneous system (ethanol-nZVI), since the samples contained various particle sizes and agglomerations exhibiting different properties.

The efficiency of Cr(VI) removal from aqueous solutions by nZVI over the 90-day period is shown in Fig. 8. The control chart illustrates that the reduction efficiency of nZVI remained stable over time. The chemical composition of the nZVI remained unchanged for several months, confirming

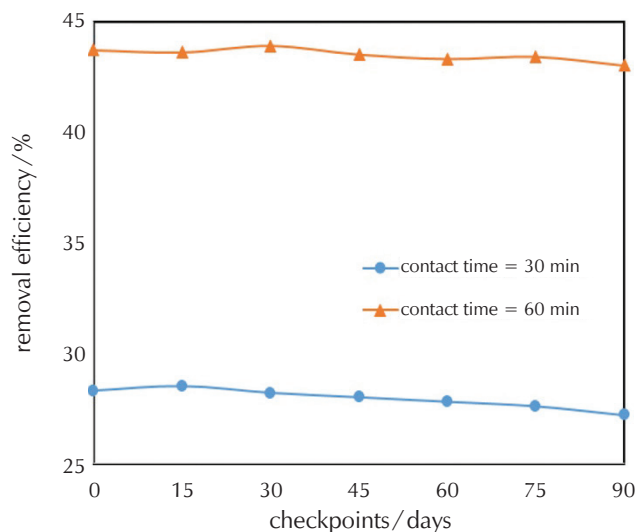


Fig. 8 – Stability check of nZVI

$C(\text{Cr(VI)}) = 2 \text{ mg l}^{-1}$, $C(\text{nZVI}) = 40 \text{ mg l}^{-1}$, $\text{pH} = 7.0$,
 $T = 20 \text{ }^\circ\text{C}$, $\omega = 1000 \text{ rpm}$

that the nZVI was properly dried and stored, and that the synthesis process was correctly modelled. The results indicated that the efficiency of Cr(VI) removal using nZVI was $27.9 \pm 3 \%$ for 30 min, and $43.5 \pm 2 \%$ for 60 min. The variations of the results are within the analytical error.

One of the primary objectives of this study was to evaluate the practical applicability of the synthesised and characterised material for the removal of Cr(VI) from model aqueous solutions. A solid powder electron-donor material was chosen for production due to its suitability for in situ remediation of contaminated groundwater. Among the several working parameters that influence the removal of Cr(VI) from aqueous solutions by nZVI, such as contact time, temperature, solution pH, Cr(VI) concentration, and nZVI concentration, the effects of contact time and initial nZVI concentration were studied. The other working parameters were held constant (Fig. 9) at values close to those found in local groundwater contaminated with Cr(VI). The efficiency of Cr(VI) removal using nZVI at different initial nZVI concentrations and fixed initial Cr(VI) concentration is given in Fig. 9.

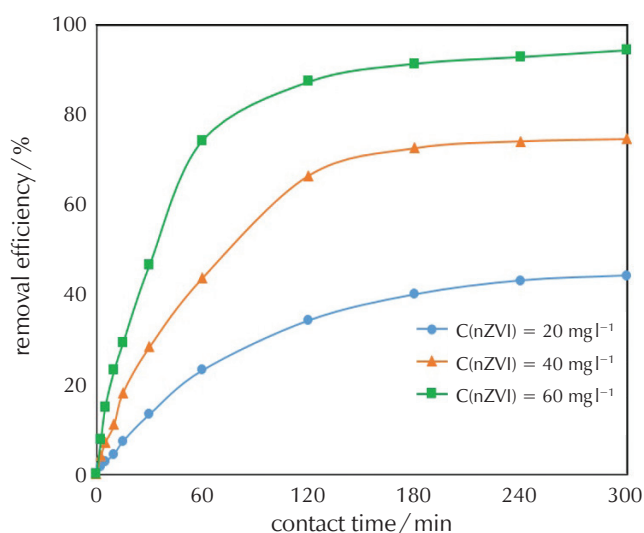


Fig. 9 – Efficiency of Cr(VI) removal from aqueous solution using nZVI
 $C(\text{Cr(VI)}) = 2 \text{ mg l}^{-1}$, $\text{pH} = 7.0$, $T = 20 \text{ }^\circ\text{C}$, $\omega = 1000 \text{ rpm}$

Three different initial nZVI concentrations were tested in the system. The kinetics of removal efficiency indicated that increasing the initial nZVI concentration led to a higher removal efficiency. During the first 120 min, the concentration of hexavalent chromium decreased significantly, followed by a slower rate of decline. The strong influence of the initial nZVI concentration on removal efficiency was possibly due to the nZVI/Cr(VI) concentration ratio. The Cr(VI) removal efficiency of nZVI was determined to be 44.2, 74.6, and 94.5 % after 300 min at constant initial

Cr(VI) concentrations of 2 mg l^{-1} and initial nZVI concentrations of 20, 40, and 60 mg l^{-1} , respectively.

The characterisation results confirmed that the synthesised material was pure nZVI, free from impurities that could further contaminate the treated water. This is particularly important from both engineering and environmental perspectives. The application of nano iron in the zero oxidation state, characterised by minimal amounts of iron oxides or hydroxides, small particle size, and large surface area, maximizes the material's potential as an absorbent and an electron donor, allowing for the use of a smaller amount of material to achieve the desired Cr(VI) removal efficiency. The process kinetics analysis suggested that the optimal removal efficiency for each investigated system (with different initial nZVI concentrations) was achieved by a contact time of 240 min. Furthermore, storing nZVI in vacuum bags is a cost-effective alternative to using inert gases or liquids, as it reduces production costs. Consequently, the synthesised material offers a low-cost, environmentally friendly, easy-to-implement, and highly efficient solution for in situ remediation of Cr(VI)-contaminated groundwater. Additionally, the synthesis procedure is well modelled and suitable for scaling up or developing industrial processes for producing large quantities of nZVI with the characteristics presented in this study.

4 Conclusion

Nano zero-valent iron was successfully synthesised through the chemical reduction of Fe(III) ions in FeCl_3 solution with NaBH_4 solution under atmospheric conditions. The synthesis process included nZVI production, separation from the reaction mixture by vacuum filtration, washing drying under vacuum, and storage. SEM photographs confirmed the nanochain morphology of the obtained nZVI, while EDS analysis verified that the iron was in the zero oxidation state. TGA results indicated that from 100 to $850 \text{ }^\circ\text{C}$, the weight of nZVI increased almost linearly, indicating the oxidation of Fe(0) to Fe(II) and Fe(III), due to the high electron-donor tendency of nZVI. The X-ray diffraction pattern confirmed the zero oxidation state of the synthesised iron and its body-centred cubic crystal structure. The obtained material was pure iron with negligible impurities (EDXRF analysis). The SSA analysis indicated a BET surface area of $23.79 \text{ m}^2 \text{ g}^{-1}$. The chemical stability tests of nZVI revealed that the chemical composition remained stable for several months. The synthesised material was used for Cr(VI) reduction. The effects of contact time and initial nZVI concentration on the process efficiency of Cr(VI) removal from aqueous solution were studied. The removal efficiency increased with higher initial nZVI concentrations at a constant initial Cr(VI) concentration. The removal efficiencies were 44.2, 74.6, and 94.5 % after 300 min at initial nZVI concentrations of 20, 40, and 60 mg l^{-1} , respectively. This study demonstrates that the prepared nZVI is effective for treating wastewater and groundwater contaminated with hexavalent chromium.

List of symbols and abbreviations

C_0	– initial concentration
C_t	– given time concentration
E^0	– standard reduction potential
C	– concentration
R	– Cr(VI) removal efficiency
T	– temperature
θ	– angle of incidence
λ	– wavelength
p	– absolute pressure
p_0	– saturation pressure
ω	– mixing speed
1D	– one-dimensional
bcc	– body-centred cubic
DTG	– differential thermogravimetry
EDS	– energy-dispersive spectrometer
EDXRF	– energy dispersive X-ray fluorescence
nZVI	– nano zero-valent iron
SDD	– silicon drift detector
SEM	– scanning electron microscopy
TG	– thermogravimetric
TGA/ DTA	– thermogravimetric/differential thermal analysis
BET	– Brunauer–Emmett–Teller
UV/Vis	– ultraviolet-visible
XRPD	– X-ray powder diffraction

References

Literatura

1. *D. Jyoti, R. Sinha, C. Faggio*, Advances in biological methods for the sequestration of heavy metals from water bodies: A review, *Environ. Toxicol. Pharmacol.* **94** (2022) 103927, doi: <https://doi.org/10.1016/j.etap.2022.103927>.
2. *B. G. Loganathan, S. Ahuja, B. Subedi*, Synthetic Organic Chemical Pollutants in Water: Origin, Distribution, and Implications for Human Exposure and Health, *ACS Symp. Ser.* **1352** (2020) 13–39, doi: <https://doi.org/10.1021/bk-2020-1352.ch002>.
3. *K. H. Vardhan, P. S. Kumar, R. C. Panda*, A review on heavy metal pollution, toxicity and remedial measures: Current trends and future perspectives, *J. Mol. Liq.* **290** (2019) 111197, doi: <https://doi.org/10.1016/j.molliq.2019.111197>.
4. *P. C. Nagajyoti, K. D. Lee, T. V. M. Sreekanth*, Heavy metals, occurrence and toxicity for plants: A review, *Environ. Chem. Lett.* **8** (2010) 199–216, doi: <https://doi.org/10.1007/s10311-010-0297-8>.
5. *S. L. Thompson, F. C. R. Manning, S.M. McColl*, Comparison of the toxicity of chromium III and chromium VI to cyanobacteria, *Bull. Environ. Contam. Toxicol.* **69** (2002) 286–293, doi: <https://doi.org/10.1007/s00128-002-0059-9>.
6. *A. Ansari, V. U. Siddiqui, M. K. Akram, W. A. Siddiqi, A. Khan, A. N. Al-Romaizan, M. A. Hussein, M. Puttegowda*, Synthesis of Atmospherically Stable Zero-Valent Iron Nanoparticles (nZVI) for the Efficient Catalytic Treatment of High-Strength Domestic Wastewater, *Catalysts* **12** (2022) 26, doi: <https://doi.org/10.3390/catal12010026>.
7. *M. A. V. Ramos, Y. Weile, X. Q. Li, B. E. Koel, W. X. Zhang*, Simultaneous Oxidation and Reduction of Arsenic by Zero-Valent Iron Nanoparticles: Understanding the Significance of the Core-Shell Structure, *J. Phys. Chem. C* **113** (2009) 14591–14594, doi: <https://doi.org/10.1021/jp9051837>.
8. *Y. P. Sun, X. Q. Li, J. Cao, W. X. Zhang, H. P. Wang*, Characterization of zero-valent iron nanoparticles, *Adv. Colloid Interface Sci.* **120** (2006) 47–56, doi: <https://doi.org/10.1016/j.cis.2006.03.001>.
9. *M. M. Tarekegn, A. M. Hiruy, A. H. Dekebo*, Nano zero valent iron (nZVI) particles for the removal of heavy metals (Cd^{2+} , Cu^{2+} and Pb^{2+}) from aqueous solutions, *RSC Adv.* **11** (2021) 18539–18551, doi: <https://doi.org/10.1039/d1ra01427g>.
10. *D. Liang, Y. Fan, T. Yue, W. Wang, Q. Shang, P. Chen, M. Zhu, Y. Liu, G. Cui, B. Tang*, Photocatalytic Activity of Zero-Valent Iron Nanoparticles Highly Dispersed on Porous Carbon Materials, *Front. Environ. Chem.* **3** (2022) 898879, doi: <https://doi.org/10.3389/fenvc.2022.898879>.
11. *D. S. Ken, A. Sinha*, Recent developments in surface modification of nano zero-valent iron (nZVI): Remediation, toxicity and environmental impacts, *Environ. Nanotechnol. Monit. Manag.* **14** (2020) 100344, doi: <https://doi.org/10.1016/j.enmm.2020.100344>.
12. *C. Jie Wei, Y. F. Xie, X. M. Wang, X. Y. Li*, Calcium hydroxide coating on highly reactive nanoscale zero-valent iron for in situ remediation application, *Chemosphere* **207** (2018) 715–724, doi: <https://doi.org/10.1016/j.chemosphere.2018.05.128>.
13. *L. Dai, K. Meng, W. Zhao, T. Han, Z. Lei, G. Ma, C. Wu, H. Jia*, Enhanced removal of Cd^{2+} by nano zero-valent iron modified attapulgite from aqueous solution: Optimal design-characterization and adsorption mechanism, *J. Environ. Chem. Eng.* **10** (2022) 107719, doi: <https://doi.org/10.1016/j.jece.2022.107719>.
14. *M. Crampon, C. Joulian, P. Ollivier, M. Charron, J. Hellal*, Shift in Natural Groundwater Bacterial Community Structure Due to Zero-Valent Iron Nanoparticles (nZVI), *Front. Microbiol.* **10** (2019) 533, doi: <https://doi.org/10.3389/fmicb.2019.00533>.
15. *A. M. Azzam, S. T. El-Wakeel, B. B. Mostafa, M. F. El-Shahat*, Removal of Pb, Cd, Cu and Ni from aqueous solution using nano scale zero valent iron particles, *J. Environ. Chem. Eng.* **4** (2016) 2196–2206, doi: <https://doi.org/10.1016/j.jece.2016.03.048>.
16. *M. M. El-Shafei, A. Hamdy, M. M. Hefny*, Zero-valent iron nanostructures: synthesis, characterization and application, *J. Environ. Biotechnol. Res.* **7** (2018) 1–10.
17. *O. Gibert, M. Abenza, M. Reig, X. Vecino, D. Sánchez, M. Araldos, J. L. Cortina*, Removal of nitrate from groundwater by nano-scale zero-valent iron injection pulses in continuous-flow packed soil columns, *Sci. Total Environ.* **810** (2022) 152300, doi: <https://doi.org/10.1016/j.scitotenv.2021.152300>.
18. *Q. Li, Z. Chen, H. Wang, H. Yang, T. Wen, S. Wang, B. Hu, X. Wang*, Removal of organic compounds by nanoscale zero-valent iron and its composites, *Sci. Total Environ.* **792** (2021) 148546, doi: <https://doi.org/10.1016/j.scitotenv.2021.148546>.
19. *W. Liang, C. Dai, X. Zhou, Y. Zhang*, Application of zero-valent iron nanoparticles for the removal of aqueous zinc ions under various experimental conditions, *PLoS One* **9** (2014) e85686, doi: <https://doi.org/10.1371/journal.pone.0085686>.
20. *Ç. Üzümlü, T. Shahwan, A. E. Eroğlu, I. Lieberwirth, T. B. Scott*,

- K. R. Hallam, Application of zero-valent iron nanoparticles for the removal of aqueous Co^{2+} ions under various experimental conditions, *J. Chem. Eng.* **144** (2008) 213–220, doi: <https://doi.org/10.1016/j.cej.2008.01.024>.
21. H. Zhu, Y. Jia, X. Wu, H. Wang, Removal of arsenic from water by supported nano zero-valent iron on activated carbon, *J. Hazard. Mater.* **172** (2009) 1591–1596, doi: <https://doi.org/10.1016/j.jhazmat.2009.08.031>.
 22. J. Ye, Y. Wang, Q. Xu, H. Wu, J. Tong, J. Shi, Removal of hexavalent chromium from wastewater by Cu/Fe bimetallic nanoparticles, *Sci. Rep.* **11** (2021) 10848, doi: <https://doi.org/10.1038/s41598-021-90414-0>.
 23. L. Li, Q. Xu, S. Li, W.X. Zhang, Wet Milling of Zerovalent Iron in Sulfide Solution: Preserving and Securing the Metallic Iron, *ACS EST Eng.* **2** (2022) 703–712, doi: <https://doi.org/10.1021/acsestengg.1c00361>.
 24. R. Nisticò, L. Carlos, High yield of nano zero-valent iron (nZVI) from carbothermal synthesis using lignin-derived substances from municipal biowaste, *J. Anal. Appl. Pyrolysis* **140** (2019) 239–244, doi: <https://doi.org/10.1016/j.jaap.2019.03.022>.
 25. R. A. Crane, T. B. Scott, Nanoscale zero-valent iron: Future prospects for an emerging water treatment technology, *J. Hazard. Mater.* **211-212** (2012) 112–125, doi: <https://doi.org/10.1016/j.jhazmat.2011.11.073>.
 26. T. Pasinszki, M. Krebsz, Synthesis and application of zero-valent iron nanoparticles in water treatment, environmental remediation, catalysis, and their biological effects, *Nanomaterials* **10** (2020) 917, doi: <https://doi.org/10.3390/nano10050917>.
 27. B. K. Khuntia, M. F. Anwar, T. Alam, M. Samim, M. Kumari, I. Arora, Synthesis and Characterization of Zero-Valent Iron Nanoparticles, and the Study of Their Effect against the Degradation of DDT in Soil and Assessment of Their Toxicity against Collembola and Ostracods, *ACS Omega* **4** (2019) 18502–18509, doi: <https://doi.org/10.1021/acsomega.9b01898>.
 28. R. Singh, V. Misra, R. P. Singh, Synthesis, characterization and role of zero-valent iron nanoparticle in removal of hexavalent chromium from chromium-spiked soil, *J. Nanopart. Res.* **13** (2011) 4063–4073, doi: <https://doi.org/10.1007/s11051-011-0350-y>.
 29. A. Boran, S. Erkan, I. Eroglu, Hydrogen generation from solid state NaBH_4 by using FeCl_3 catalyst for portable proton exchange membrane fuel cell applications, *Int. J. Hydrog. Energy* **44** (2019) 18915–18926, doi: <https://doi.org/10.1016/j.ijhydene.2018.11.033>.
 30. M. R. Jamei, M. R. Khosravi, B. Anvaripour, Investigation of ultrasonic effect on synthesis of nano zero valent iron particles and comparison with conventional method, *Asia-Pac. J. Chem. Eng.* **8** (2013) 767–774, doi: <https://doi.org/10.1002/apj.1720>.
 31. B. Desalegn, M. Megharaj, Z. Chen, R. Naidu, Green synthesis of zero valent iron nanoparticle using mango peel extract and surface characterization using XPS and GC-MS, *Heliyon* **5** (2019) e01750, doi: <https://doi.org/10.1016/j.heliyon.2019.e01750>.
 32. S. Eslami, M. A. Ebrahimzadeh, P. Biparva, Green synthesis of safe zero valent iron nanoparticles by: Myrtus communis leaf extract as an effective agent for reducing excessive iron in iron-overloaded mice, a thalassemia model, *RSC Adv.* **8** (2018) 26144–26155, doi: <https://doi.org/10.1039/c8ra04451a>.
 33. G. Kozma, A. Rónavári, Z. Kónya, Á. Kukovecz, Environmentally Benign Synthesis Methods of Zero-Valent Iron Nanoparticles, *ACS Sustain. Chem. Eng.* **4** (2016) 291–297, doi: <https://doi.org/10.1021/acssuschemeng.5b01185>.
 34. R. Yuvakkumar, V. Elango, V. Rajendran, N. Kannan, Preparation and characterization of zero valent iron nanoparticles, *Digest J. Nanomater. Biostruct.* **6** (2011) 1771–1776.
 35. X. Q. Li, W. X. Zhang, Iron nanoparticles: The core-shell structure and unique properties for Ni(II) sequestration, *Langmuir* **22** (2006) 4638–4642, doi: <https://doi.org/10.1021/la060057k>.
 36. C. Wang, D. R. Baer, J. E. Amonette, M. H. Engelhard, J. Antony, Y. Qiang, Morphology and electronic structure of the oxide shell on the surface of iron nanoparticles, *J. Am. Chem. Soc.* **131** (2009) 8824–8832, doi: <https://doi.org/10.1021/ja900353f>.
 37. A. Polman, H. A. Atwater, Plasmonics: Optics at the nanoscale, *Mater. Today* **8** (2005) 56, doi: [https://doi.org/10.1016/S1369-7021\(04\)00685-6](https://doi.org/10.1016/S1369-7021(04)00685-6).
 38. A. C. Quevedo, E. Guggenheim, S. M. Briffa, J. Adams, S. Lofts, M. Kwak, T. G. Lee, C. Johnston, S. Wagner, T. R. Holbrook, Y. U. Hachenberger, J. Tentschert, N. Davidson, E. Valsami-Jones, UV-Vis Spectroscopic Characterization of Nanomaterials in Aqueous Media, *J. Vis. Exp.* **176** (2021) e61764, doi: <https://doi.org/10.3791/61764>.
 39. Q. Shao, H. Lin, M. Shao, Determining Locations of Conduction Bands and Valence Bands of Semiconductor Nanoparticles Based on Their Band Gaps, *ACS Omega* **5** (2020) 10297–10300, doi: <https://doi.org/10.1021/acsomega.9b04238>.

SAŽETAK

Sinteza i karakterizacija nano nula valentnog željeza za redukciju i imobilizaciju Cr(VI) u vodnim resursima

Martin Stojchevski,^{a*} Stefan Kuvendziev,^a Zoran Bozinovski,^b Petre Makreski,^c
Perica Paunović,^a Mirko Marinkovski^a i Kiril Lisichkov^a

Nano nula valentno željezo (nZVI) sintetizirano je redukcijom Fe(III) koristeći otopinu željezova(III) klorida i natrijeva borohidrida pri atmosferskim uvjetima. Strukturna i kemijska karakterizacija nZVI provedena je pretražnom elektronskom mikroskopijom (SEM), rendgenskom difrakcijom praha (XRPD), rendgenskom fluorescencijom uz disperziju energije (EDXRF), termogravimetrijskom/diferencijalnom termičkom analizom (TGA/DTA), analizom specifične površine (SSA) i UV/Vis spektroskopijom. Sintetizirane nZVI čestice s kubičnom kristalnom strukturom ostale su kemijski stabilne nekoliko mjeseci. Srednji promjer nanočestica bio je manji od 60 nm uz SSA od 23,79 m² g⁻¹. Sintetizirani nZVI primijenjen je za katalitičku redukciju Cr(VI) u vodenoj otopini. Ispitan je utjecaj vremena kontakta i početne nZVI koncentracije na učinkovitost uklanjanja Cr(VI) iz vodene otopine. Nakon 300 min, učinkovitost uklanjanja dosegla je 44,2, 74,6 i 94,5 % za početne nZVI koncentracije od 20, 40, odnosno 60 mg l⁻¹. Ova studija ukazuje da je dobiveni nZVI ekološki prihvatljiv i učinkovit redukcijski agens za obradu otpadnih i podzemnih voda onečišćenih šesterovalentnim kromom.

Ključne riječi

Nano nula valentno željezo, sinteza, karakterizacija, uklanjanje Cr(VI)

^a Ss. Cyril and Methodius University in Skopje, Faculty of Technology and Metallurgy, Ulica Rugjera Boskovicica 16, 1000 Skopje, Sjeverna Makedonija

^b Eko Bio Link, Ulica Petra Deljana 3-1/4, 1000 Skopje, Sjeverna Makedonija

^c Ss. Cyril and Methodius University in Skopje, Faculty of Natural Sciences and Mathematics, Institute of Chemistry, Arhimedova ulica 5, 1000 Skopje, Sjeverna Makedonija

Izvorni znanstveni rad
Prispjelo 21. srpnja 2024.
Prihvaćeno 14. kolovoza 2024.